Adhesion energy modulation acts as an NGF receptor activator for neuronal differentiation in NGF-free medium

Océane Sénépart, Claire Legay, Christophe Hélary, Ahmed Hamraoui

Adhesion energy modulation acts as an NGF receptor activator for neuronal differentiation in NGF-free medium

Océane Sénépart[1,2], Claire Legay[2], Christophe Helary[*,2], and Ahmed Hamraoui[†1,3]

[1]Sorbonne Université, CNRS, UMR7574, Laboratoire de Chimie de la Matière Condensée de Paris, 4 place Jussieu, 75005 Paris, France
[2]CNRS UMR 8003, Université Paris Cité, Faculté des Sciences Fondamentales et Biomédicales, 45 rue ds Saints-Pères, 75006 Paris, France
[3]Université Paris Cité, Faculté des Sciences Fondamentales et Biomédicales, 45 rue des Saints-Pères, 75006 Paris, France

Abstract

Neuronal repair is promoted after a nerve injury by chemical and physical stimuli from their environment. Among them, local adhesion energy gradients generated on surfaces trigger cone formation and neurite outgrowth without any nerve growth factor (NGF) addition. In this study, the molecular mechanisms leading to neuronal differentiation after stimulation via energy gradients are investigated. For this purpose, PC12 cells are cultured on n-[3-(trimethoxysilyl)propyl] ethylen- diamine (EDA) and n-hexyl trimethoxysilane (HTMS), two functionalized surfaces possessing local energy gradients but chemically different. These surfaces similarly trigger neurite and growth cone formation after 3 days in culture. Gene expression of PI3/Akt quantified through a microarray and the action of a specific inhibitor of the corresponding pathway reveal that PI3/Akt signaling pathway is induced and activated on these surfaces in the same way as NGF does after binding on its TrkA receptor. The biological downstream effectors of this signaling pathway are also upregulated, thereby promoting cell survival, growth cone formation and neurite outgrowth. EDA and HTMS surfaces act as an ongoing stimulus of the TrkA receptor as the addition of 100 nM K252a, its specific inhibitor, leads to the inhibition of neurite growth. Taken together, these results suggest that functionalized surface with energy surface gradients could be useful to promote nerve repair after an injury.

1 Introduction

The initiation and guidance of a neurite outgrowth rely on extracellular signals originating from their microenvironment. Among them, the nanoscale topography drastically impacts the neuron interactions with their substrates, thereby controlling the cell behavior and differentiation [1–6]. Besides, gradients of soluble factors, including calcium [7, 8] and neurotrophic factors [9–11] also influence neurite out- growth through the growth cone. This specific structure, located at the tip of the neurite recognizes and transduces a combination of signals into a specific trajectory towards target cells.

More recently, our group have shown that the adhesion energy of the substrate and its spatial distribution play a crucial role in nerve regeneration. [3, 4] A combination of physico-chemical factors from the substrate such as elasticity and adhesion energy have recently been proposed to control the shape and functions of cells and tissues. [12] Therefore, it is relevant to identify the appropriate characteristics of the substrates that can efficiently promote neurite extension, a process of neuronal differentiation. [3,4,13–15] Some self-assembled monolayers (SAMs) made of alkylsiloxanes grafted on glass combine properties at the nanoscale level such as distinct surface energy distributions. At larger scale, macroscopic surface characteristics such as wettability are efficient for controlling cell adhesion, and in particular for controlling neuronal cell differentiation. [16–19]

[*] Corresponding author
[†]Corresponding author: ahmed.hamraoui@sorbonne-universite.fr

PC12 cells are well-defined models for studying the mechanisms of neuronal differentiation, and axonal regeneration thanks to their capacities: (i) to express the transmembrane receptors TrkA and p75 for the nerve growth factor (NGF) [20, 21] and (ii) differentiate into a neuronal phenotype in the presence of appropriate NGF concentrations . [3, 4, 22] NGF addition to the culture medium triggers differentiation either by activating the synthesis of proteins associated with the actin/microtubule cytoskeleton, including Tau [23, 24] and MAP1B [24], and by activating signaling pathways, mainly the PI3K-Akt or the NF-KB ones. [25] Several key inducers of neuronal differentiation of PC12 cells in medium without NGF have been identified. The neuritogenesis of PC12 cells is observed on soft substrates composed of extracellular matrix (ECM) proteins such as a combination of different collagen types associated with proteoglycans, glycosaminoglycans, fibronectin and laminin [26] or ECM derived from astrocytes . [27] Last, the neurite growth can be observed in NGF-free medium when PC12 were cultured on electroactive surfaces or after electric stimulation. [28–30]

As described in our previous studies, a surface chemically modified with alkylsiloxanes such as EDA and HTMS (see Table S1 in Supporting Information) generates local adhesion energy gradients. The energy of adhesion is the energy of cohesion between two different phases. This spatial distribution of adhesion energy (gradients) also acts as an initiator of the differentiation of PC12 cells leading to neurite and growth cone formation. [3, 4, 31] The influence of a gradient at large scale ($4.24\ mm \times 4.24\ mm$) in surface energy was also studied by Murnane [32], and showed that PC12 neurites are preferentially initiatedthe in directions of varying energy of adhesion, under NGF treatment. Other studies showed that the topography of the underlying culture substrate, at smaller scales (μm), acts in cooperation with NGF to modulate neuritogenesis in PC12 cells. [33,34] We demonstrated in our previous studies [3,4,31] the ability of PC12 cells to differentiate when seeded on solid glass substrates coated with CH_3 or NH_2 terminated SAM alkylsiloxane in medium without NGF. These surfaces contained a nanoscale mixture of hydroxyl and CH_3 (HTMS surface) or NH_2 (EDA surface) groups that generate local surface energy gradients. Despite differences in gradient values and chemical nature EDA and HTMS promoted the same neuronal differentiation.

In this study, the underlying molecular mechanisms that lead to PC12 differentiation stimulated by physical signals, *i.e* gradients of surface energy, have been elucidated. For this purpose, a microarray comparing the gene expression of PC12 cells cultivated on functionalized surface (EDA or HTMS) with that of cells cultivated on surfaces coated with biopolymers has been performed. We demonstrate that the nanoscale surface energy distribution activates the TrkA receptor, as NGF does. These results are confirmed by the negative impact of a TrkA inhibitor on neuritogenesis of PC12 cultured on functionalized surface.

2 Materials and methods

2.1 Chemicals :

Chemicals were obtained from Acros Organics (Geel, Belgium), Sigma-Aldrich (St. Quentin Fallavier, France), ABCR (Karlsruhe, Germany), Fisher Scientific (Illkirch, France) and Carlo Erba Reagents (Val de Reuil, France). The sources and purity of the chemicals used are summarized in Table 1 in the Supporting Information section.

2.2 Substrate modifications :

All chemicals were used without any additional purification. Prior to their use, glass coverslips ($30\ mm$ in diameter and $100\ \mu m$ thick, from Menzel-Glazer) were treated as follow. They were cleaned for $20\ min$ in ultrasonic bath with $CHCl_3$, followed by an immersion in piranha solution ($3:1(v/v)$ concentrated sulfuric acid and 40% hydrogen peroxide) (caution: piranha solution is extremely corrosive and can react violently with organic compounds). Then, extensive rinses in deionized water were performed. Last the glass coverslips were dried under a nitrogen stream. Modified surfaces were obtained by incubation of clean glass coverslips into a 2% EDA solution ~~dur ing~~ for $24\ h$, at room temperature in an ambient atmosphere. They were then rinsed in methanol, then dried under a nitrogen stream, (for AFM characterization) [3], or in a laminar flow cabinet (for cell culture). EDA formed “patches” by self-

polymerization on glass coverslip, due to an excess of water, here 4%, compared to the amount required for the reaction between EDA and the silica. [35, 36]

Liquid	σ	σ^d	σ^{nd}
Water	72.8	21.8	51
Glycerol	64	34	30
Formamide	58	39	19
n-Hexadecane	27.47	27.47	0
Tetradecane	26.56	26.56	0

Table 1: Values of the surface tension σ, mNm^{-1} of some test liquids at $20^{\circ}C$ (adapted from Ref. [41]. σ^d and σ^{nd} are respectively the dispersive and the polar components of the surface tension.

Beside EDA, an other trialkoxysilane, the HTMS was used to modify clean glass coverslips, using the same method. Control surfaces were prepared by coating glass coverslips with PLL (Poly-L-lysine) biopolymer.

2.3 Contact angle measurements :

Contact angles (θ) were measured using liquids listed in **Table 1** according to the procedures described in Refs. . [3, 4, 37] The method of measuring the contact angle at a liquid / solid interface consists of snaping an image of a liquid drop deposited on a solid surface using a high-resolution camera. In this work, we used a drop shape analyzer apparatus DSA30 from Krüss. The image was then processed with the included software which calculates the contact angle value from the profile of the drop using the Young-Laplace method. At least 3 drops of each liquid, per sample, were analyzed.

2.4 Determination of surface free energy :

The critical surface tension σ_c was calculated using the Fox-Zisman approximation. In this study, it can be considered as a first-order approximation of the Good-Girifalco equation [38], for a surface tension of the liquid σ_L (σ_L ≥) close to the σ_c of the solid. Using a linear regression analysis, Zisman plots, $\cos(\theta) = f(\sigma_L)$ were traced for each substrate by fitting the data obtained with the test liquids. σ_c values were read where the line fits intersect $\cos(\theta) = 1$, as described by Zisman.[39].

Using the measured contact angles, the surface free energies (SFE) for the two substrates (EDA and HTMS) were determined. Using the Owens-Wendt theoretical model [40], the long-range dispersive (Lifshitz-Van der Waals; σ^d) and the short-range non-dispersive (example: hydrogen bonding, acid-base interactions, ...) σ^{nd}) components of SFE were calculated according to the following equation:

$$W_{SL} = \sigma_L(1 + \cos\theta) = 2\left(\sqrt{\sigma^d\sigma_s^d} + \sqrt{\sigma^{nd}\sigma^{nd}_L}\right) \quad (1)$$

where σ_S is the SFE of the surface, σ_L is the SFE of the liquid and W_{SL} is the solid-liquid energy of adhesion. In Equation 1, we have two unknown parameters, namely σ^d_s and σ^{nd}_s. Then, we need to build two equations from equation 1. That is why two values of contact angles were chosen as probes for SFE calculations: n-hexadecane, and H_2O. For a liquid, the overall surface tension (σ_L) is a combination of dispersive and polar components, whose values are indicated in Table 1 (adapted from Ref. [5]). The contact angles of n-hexadecane and H_2O were reported in Equation 1 for each solid substrate, then sample SFE components were calculated.

To measure the advancing and receding contact angles, the volume of the drop was increased and de-creased. After the drop volume increased/decreased and the triple line (periphery) advanced/receded on the surface, the advancing/receding contact angle was measured and the measurement was per- formed within 10 to 15 seconds after. The average volume used to perform the measurements is approximately 0.05 mL. Care was taken to minimize drop vibration and distortion during volume changes. Angles were measured on four to six different regions of each surface and averaged. Repro- ducibility for any given region was $\pm 2^{\circ}$.

		PC12 cultivated on		
		PLL	EDA	HTMS
Control →		X	X	X
	NGF 100 *ng mL*$^{-1}$	X		
When seeding or 24h after seeding	K252a 10 *nM*	+NGF	X	X
	K252a 100 *nM*	+NGF	X	X

Table 2: Description of the protocol over time for the two experiments. They were carried out, one on day 0 and the second on day 1. For each experiment, both concentrations of the inhibitor K252a were used, *i.e.* 10 *nM* and 100 *nM* . In total, four sets of experiments were carried out. X = Done

2.5 PC12 cell culture on modified surfaces:

PC12 cells, a standard model for neuronal differentiation analysis [22], were obtained from ATCC (CRL 1721). Cells were expended in T25 tissue culture flasks (Falcon) coated with PLL, using medium 1, *i.e.* DMEM + glutamax supplemented with Fetal Bovine Serum FBS (5%, Hyclone), horse serum (HS) (10%, Invitrogen), non-essential amino acids (1%, Invitrogen) and antibiotic (penicillin, streptomycin) (1%, Invitrogen) at 37° C in a 5%CO_2 atmosphere. Media were changed every 2-3 days. Subculturing was done when 90% of confluence was reached, by trypsin-EDTA treatment (Invitrogen) to detach cells and seed them at 20% of confluence into new flasks. PC12 cells were used between passage 7 and 17 at a density of 5.10^3 cm^{-2}. for the experiments on glass coverslips functionalized with EDA or HTMS. Medium 1 without HS (medium 2) was used to slow down cell proliferation. Coverslips were placed into plastic Petri dishes (30 *mm* in diameter) and 5.10^4 cm^{-2} cells were then seeded per dish. PC12 cultured on PLL coated coverslips were used as negative control. The addition of NGF (100 *ng* mL^{-1} , NGF-7S, from the submandibular glands of mice) into the medium 1 of PC12 cultivated on PLL was used as positive control to trigger neurite outgrowth. In each condition, cell morphology was daily observed over 3 days using an inverted light microscope (Olympus CKX41).

2.6 PC12 cell culture on modified surfaces in the presence of K-252a, a high-affinity nerve growth factor receptor blocker:

PC12 cells were seeded onto surfaces modified with EDA or HTMS or on surfaces coated with PLL using medium 1. Then, the NGF receptor inhibitor K-252a, diluted in medium 1 was added after 5 minutes or 24 hours later post seeding. Two different inhibitor concentrations were used for each modified surface, *i.e* 10 *nM* and 100 *nM* . PC12 cultured on surfaces without inhibitor were used as controls to evaluate the inhibitory effect of K-252a. Positive controls were performed and added to the set of experiments. For this purpose, PC12 were cultured on PLL over 3 days in medium 1 supplemented with 100 *ng* mL^{-1} NGF and K-252a concentrated at 10 or 100 *nM* (all the conditions are listed in **Table 2**). After 24 h, medium 1 was replaced by medium 2 in presence of inihibitor or not. The effect of K-252a on neurite growth was assessed at day 3 by live microscopy using an Olympus microscope.

2.7 RNA extraction :

Total RNAs were extracted from PC12 cells cultivated for 3 days on the different surfaces (EDA, HTMS or PLL) using a variant of Trizol. PC12 culture on PLL in presence of NGF was used as a positive control for neural differentiation. Briefly, 1 *mL* of TriReagent (Invitrogen) was added onto cells, then lysates were collected into 1.5 *mL* microfuge tubes. Phase separation was performed by adding chloroform (0.2 *mL*, Sigma-Aldrich), and total RNA was purified using an RNeasy kit (Qiagen), according to the supplier's recommended procedure. Total RNA quantity and purity were determined using an ultraviolet spectrophotometer (NanoDrop ND-1000 Spectrophotometer, NanoDrop Technologies). RNA integrity was checked electrophoretically using the RNA 6000 Nano LabChip kit on Agilent Bioanalyser 2100 (Agilent Technologies). Then RNAs were stored at $-80^{\circ}C$ prior to utilization.

2.8 Gene expression of NGF :

A fraction of RNAs from different conditions was reverse transcribed into complementary DNA (cDNA) using M-MLV RT enzyme (Life Technologies) at $37^{\circ}C$ for 1 hour. Then the enzyme was inactivated at $70^{\circ}C$ for 15 *min*. Nerve growth factor (NGF) gene expression was quantified using real-time reverse transcriptase PCR (RT-qPCR) in a Light Cycler 480 system (Roche) using the Light Cycler FastStart DNA Master plus SYBR Green I kit (Roche) ($n = 3$). mRNA levels were normalized with the housekeeping gene Mrpl9. Appropriate primers for RT-qPCR are listed in supporting information (Table 2 in Supporting Information). Cycling conditions were the following: cDNAs were denaturated at $95^{\circ}C$ for 5 min prior to 40 cycles, each cycle consisting of 10 *s* denaturation at $95^{\circ}C$; 15 s annealing at $60^{\circ}C$ and 15 s elongation at $72^{\circ}C$. Then, a melting curve was obtained by increasing the temperature from $60^{\circ}C$ to $97^{\circ}C$ at a rate of $0.1^{\circ}C/s$ to assess the reaction specificity. The results were analyzed using a relative quantification following the Pfaffl method . [42]. The efficiency of the target and reference primer pairs was measured by producing a standard curve based on the amplification of a serial dilution of cDNA. Then, a ratio was calculated by comparison with a calibration point which was the gene expression of NGF from PC12 cells cultivated on surfaces coated with PLL. The value 1 was arbitrary given to this calibration point. Results are presented as the mean relative expression with standard deviation. Statistical differences were evaluated using the Mann-Whitney test.

2.9 Microarray:

The Affymetrix ClariomS Rat array data set were obtained using Expression console (Affymetrix) and further analyses and visualization were made using EASANA (GenoSplice, www.genosplice.com), which is based on the FAST DB 2018-1 annotations. [43, 44] Gene Array data were normalized using quantile normalization. Background corrections were made with antigenomic probes which were selected as described previously. [45] Only probes targeting exons annotated from FAST DB transcripts were selected to focus on well-annotated genes whose mRNA sequences are in public databases. [43, 44] Bad-quality selected probes (e.g., probes labeled by Affymetrix as 'cross-hybridizing') and probes whose intensity signal was too low compared to antigenomic background probes with the same GC content were removed from the analysis. Only probes with a DABG p value ≤ 0.05 in at least half of the arrays were considered for statistical analysis. [45] Only genes expressed in at least one compared condition were analyzed. To be considered to be expressed, the DABG p value had to be ≤ 0.05 for at least half of the gene probes. We performed an unpaired Student's t-test to compare gene intensities in the different biological replicates. Genes were considered significantly regulated when fold-change was ≥ 1.5 and P value ≤ 0.05. Significant KEGG pathways [45], REACTOME pathways [46] and GO terms were retrieved using DAVID [47] from all the results, up- and down-regulated genes separately.

2.10 Immunofluorescence

PC12 cells were fixed for 10 *min* with a freshly made 4% paraformaldehyde solution and then permeabilized for 10 *min* in PBS-Triton (0.25% *v/v*). After 3 extensive washes in PBS, cells were incubated in a blocking solution (PBS-Triton, 1% albumin, 10% horse serum) for one hour and then incubated overnight at $4^{\circ}C$ with primary antibodies. Antibodies anti α-tubulin (dilution 1/200) and anti GAP43 (dilution 1/200) were purchased from Sigma-Aldrich and Abcam respectively. The following day, cells were rinsed with PBS 3 $\times$ 10 *min* and incubated for 90 *min* at room temperature with secondary an- tibodies diluted in the blocking solution. For α-Tubulin, a mouse anti-rabbit, Alexa 488 (Invitrogen) was used and a goat anti-mouse, Alexa 488 (Thermofisher) was used for GAP43. After this step, cells were washed 3 X10 *min* in PBS. Phalloidin, Alexa 488 (Thermofisher) was used to label actin (dilution 1/200). After the permeabilization step, cells were incubated for 45 *min* in the Phalloidin solution. Then, cells were rinsed 3 X10 *min* in PBS. Last, for each condition, cells were incubated in DAPI (1/5000 in PBS) for 10 *min* to visualize nuclei, rinsed in PBS (3 X 10 *min*) and observed with a fluorescence microscope (Zeiss Axio Observer D1).

2.11 Statistical analysis :

All the experiments were carried out with six replicates and the results expressed as the mean values ± standard deviation (SD). The statistical differences were analyzed using a Mann-Whitney test, $p < 0.05$

was considered significant. For this analysis, the software Excel Stat was used.

3 Results

3.1 Surface energy of functionalized surfaces

The data obtained for the contact angles (**Table 3**) make it possible to determine the free surface energy. The surface tensions of each substrate ($R\,NH_2$ and $R\,CH_3$) are mainly composed of dispersive and non-dispersive contributions (the latter is sometimes called polar). On the surface, modified with HTMS, thanks to the disorder in the surface grafted layer, the few exposed hydroxyl groups generate a higher non-dispersive contribution to the surface energy $\sigma^{nd} \geq 20.9\ mN\ m^{-1}$. The values of $\sigma^{HTMS}_{c} \approx 27\ mJ\ m^{-2}$ and $\sigma^{EDA}_{c} \approx 40\ mJ\ m^{-2}$, determined by Zisman plots (**Figure 1**) are in agreement with that determined previously [3, 4, 37, 48]. In the case of HTMS surfaces, σ^{HTMS}_{c} can be assimilated to σ^{d} and the ratio between $\frac{\sigma^{nd}}{\sigma_{d}} \approx 0.77$ which represents 43% of surface total energy of the surface modified using HTMS. For modified surfaces using EDA, the surface energy is partitioned as follow: $\frac{\sigma^{nd}}{\sigma_{d}} \approx 0.18$ which represents 18% of surface total energy of the surface modified using EDA.

Liquid	Surface Tension ($mN\ m^{-1}$)	Contact Angle (Degrees)	
		HTMS	EDA
Water	72.8	74.2	49.9
Glycerol	64	75	42
Formamide	58	59.3	30.55
Diodomethane	50.8	54.95	32.5
Bromonaphtalene	44.4	37.9	14.2
N-Hexadecane	27.47	11	

Table 3: Contact angle values measured on surfaces modified with HTMS and EDA.

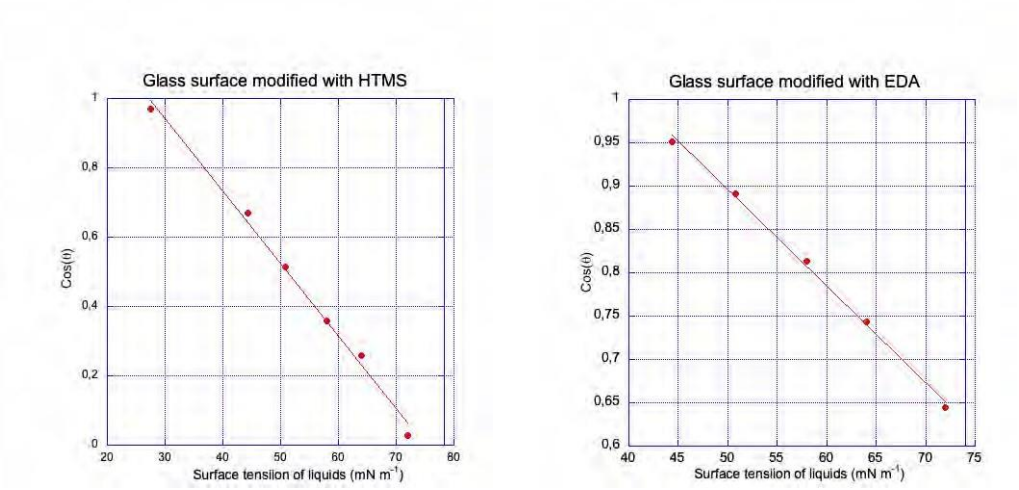

Figure 1: Zisman plots used to determine the critical surface tension (σ_c) of solid substrates. (Left) surface modified with HTMS (Right) surface modified with EDA, σ_c values were read where the line fits intersect $\cos\theta = 1$ (numerical values are displayed in Table 3).

In order to estimate the adhesion energy of water on functionalized surfaces, the contact angle on the SAM of HTMS on glass is measured and is equal to $\theta_{water} = 104^{\circ}$, which leads to an adhesion energy of $55.2\,mJ\,m^{-2}$. The difference between the adhesion energies on glass-HTMS and on clean glass is : $\Delta E = W_{glass} - W_{HTMS} = 90.4\ mJ\ m^{-2}$, where $W_i = \sigma_{water}(1 + \cos\theta_i)$, (i= glass, EDA or HTMS) is the energy of adhesion of water on substrate i. The energy of adhesion of water on clean glass is $145.6\ mJ\ m^{-2}$. Previously [4], we had estimated the difference in adhesion energy between the glass and the modified glass-EDA surface. We have found that $\Delta W_{EDA} \approx 61\ mJ\ m^{-2}$ is less superior than that of Glass-HTMS Modified Surface. This is normal because HTMS gives the surface a hydrophobic character, while EDA gives the surface a hydrophilic character. It is quite logical that we find $\Delta W_{HTMS} > \Delta W_{EDA}$.

This difference in the surface fraction of energy is in perfect agreement with the estimations of the differentials in adhesion energy between the two domains grafted on the surfaces $R\ CH_3$ or $R\ NH_2$ and OH. –

Another physical parameter which has a significant influence on the behavior of the cell is the roughness of the surface. This parameter ($\Delta\theta$) is estimated here by the conventional method of the difference between the contact angles of advancing (θ_a) and receding (θ_r) of a drop of water.

$\Delta\theta = \theta_a - \theta_r$ values are 11° and 17.5° for surfaces modified by HTMS and EDA respectively. The hysteresis of the contact angle can also be the signature of the presence of a chemical heterogeneity of the surfaces, which is the case here. [49].

3.2 PC12 cell culture on modified surfaces

We carried out cell culture experiments of PC12 on different surfaces: on Poly-L-lysine (PLL) with and without the addition of NGF to the medium, on glass-EDA surface and on glass-HTMS surface. Results are shown on **Figure 2**. PC12 cells cultivated on PLL with NGF (see Figure 4c in [3]), on glass-EDA surface in NGF-free medium and on glass-HTMS surface in NGF-free medium developed neurites. However, when the same cells are cultivated in the same conditions (without NGF) but on a PLL substrate, no neurite development process was observed, suggesting that the cells did not differentiate on this substrate. The average neurites' size of the PC12 cells cultivated on PLL without NGF does not appear on Figure 2 because of the insignificant number of neurites that did not allow us to calculate an accurate mean (**Figure 3**).

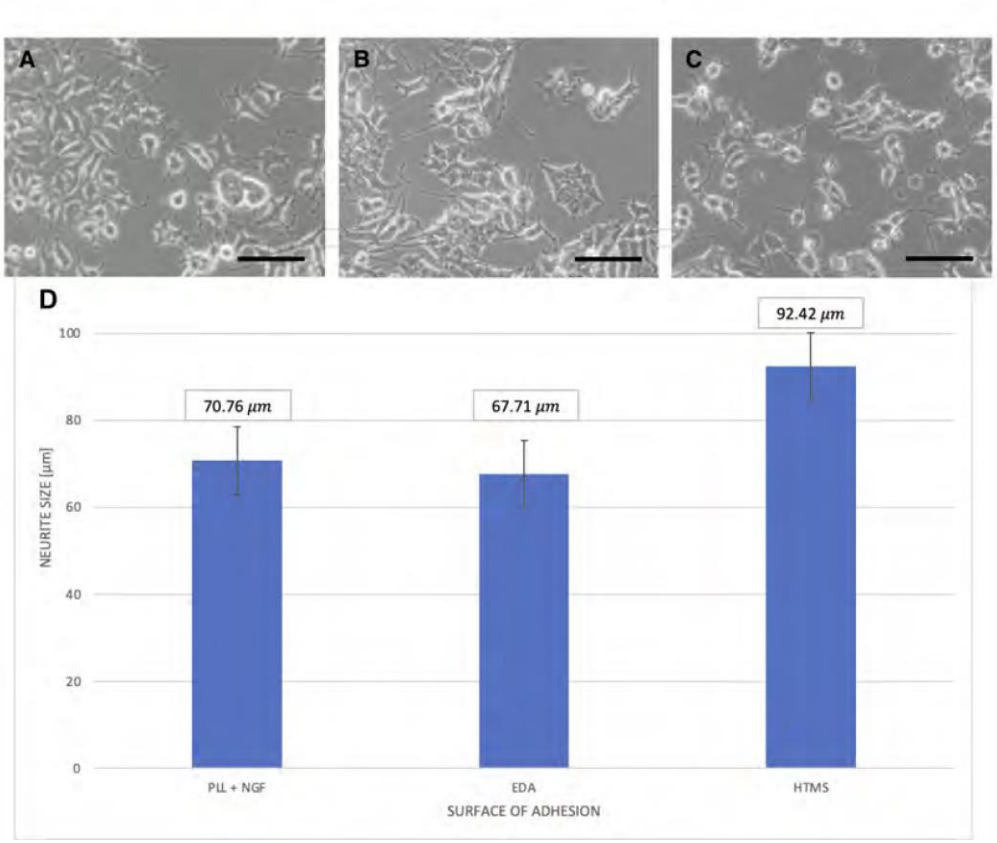

Figure 2: (A-C) PC12 cells cultured for 3 days on a PLL coating with NGF addition (A), on glass-EDA surface (B) and on glass-HTMS surface (C). HTMS and EDA = terminated CH_3 and NH_2 molecule respectively. Bar : 50 μm. In panel D are shown the neurite lengths of PC12 cells cultivated on the different surfaces: on PLL in the presence of NGF, on EDA and HTMS.

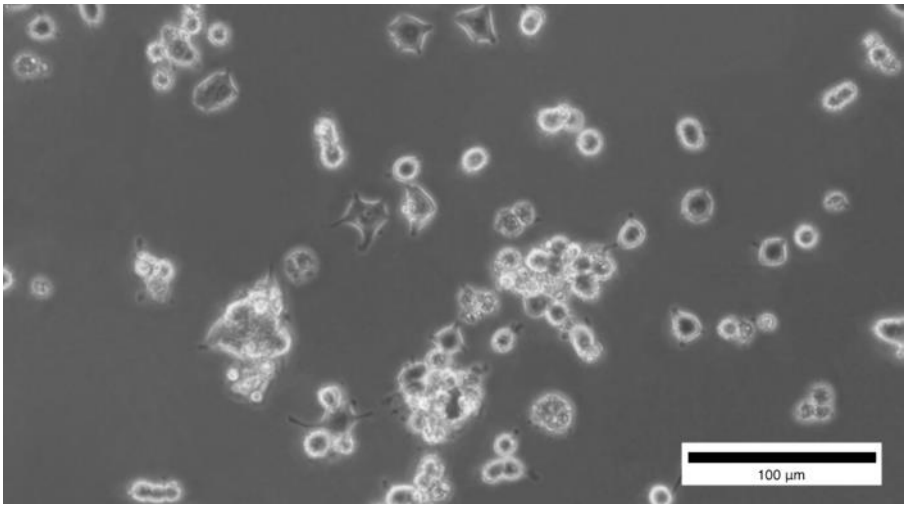

Figure 3: PC12 cells cultured on PLL surface without NGF.

3.3 NGF expression on EDA and HTMS

Nerve Growth Factor (NGF) mRNAs were measured in PC12 cells cultured on the different functionalized surfaces (HTMS and EDA) and compared to that of cells cultivated on Poly-L-lysine (used as negative control). This quantification was performed after 72 hours in culture when neurites were observable in PC12 cells when cultured on EDA and HTMS. As seen in **Figure 4**, the neurite outgrowth was not associated with an upregulation of the NGF gene expression as no significant difference was observed ($p > 0.05$, Mann-Whitney test).

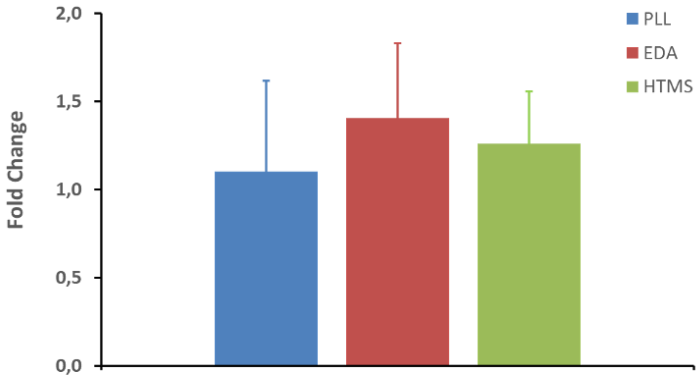

Figure 4: NGF mRNA levels in PC12 cells cultivated on the different functionalized surface.

3.4 Gene expression profile of PC12 cells cultivated on the different functionalized surfaces

The comparison of the PC12 gene expressions cultivated on the different surfaces was performed after 3 days in culture when the neurites were formed on HTMS and EDA without the addition of NGF. From the microarray values, gene expression was considered regulated only if the fold change was more than 1.5 with $p \leq 0.05$. On the EDA surface, the neurite outgrowth was associated with the upregulation of 2121 genes and the downregulation of 1215 other genes (3336 regulated genes in total). Similarly, the neurite growth on HTMS surface triggered the regulation of 2669 genes. Among them, 1777 were

upregulated and 892 were downregulated (**Figure 5**). When the gene expression of PC12 cultivated on HTMS was compared to that of cells cultivated on EDA, only 76 genes were regulated (38 upregulated and 38 downregulated). This shows that PC12 cultivated on EDA and HTMS have a similar gene

expression profile. A comparison between gene expression of PC12 cultivated on PLL + NGF and PLL without NGF was performed. After 3 days in culture and neurite formation, only 23 genes were regulated (18 upregulated and 5 downregulated), suggesting that the effect of NGF at mRNA levels was finished because all the signaling pathways leading to neurite formation are not activated anymore. On the opposite, the contact of PC12 cells with HTMS and EDA acts as an ongoing stimulus leading to a dramatic gene expression regulation.

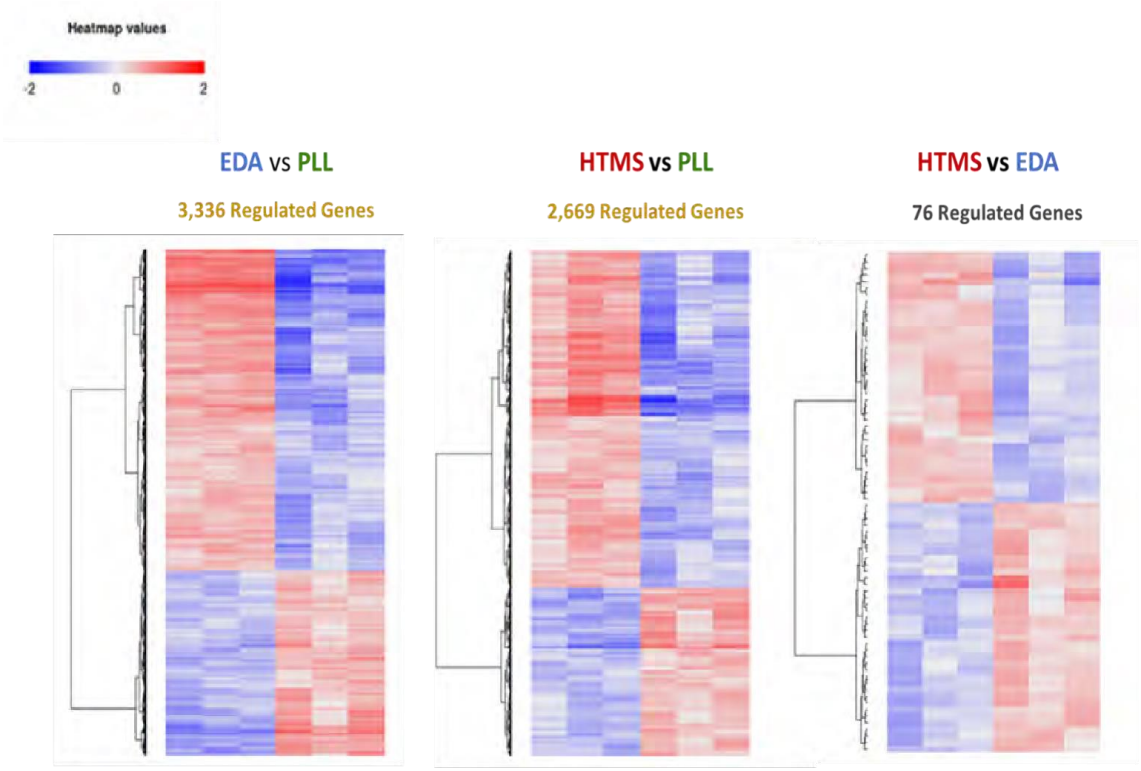

Figure 5: Hierarchical Clustering of Regulated Genes. Comparison of gene expression between EDA and PLL, HTMS and PLL, HTMS and EDA. Values taken into account: Fold-change 1.5 and $p \geq \leq 0.05$. $n = 3$ for each group.

3.5 Regulation of signaling pathways on EDA and HTMS

The fine analysis of the microarray revealed the upregulation of 47 genes involved in the PI3K-Akt signaling pathways when PC12 cells were cultivated on EDA surface (**Table 4**). No gene was downregulated. PI3K-Akt is the main signaling pathway induced by NGF through TrkA, its membrane receptor. This usually leads to neuron differentiation and neurite outgrowth. Overall, the neurotrophin signaling pathways were upregulated with 27 genes upregulated vs 10 downregulated. The Toll like receptor signaling pathways were also activated with 17 upregulated genes. Interestingly, the Toll-like receptor R4 TlR4 is upregulated (3.4 fold). The activation of TlR4 is connected to the PI3K-Akt pathway. In addition, the activation of TlR4 can lead to the expression of NF-kB, transcription factor involved in cell survival. The ErbB signaling pathway, another signaling pathway leading to the activation of the PI3K-Akt one is activated with 27 genes upregulated vs 9 downregulated (Table 4). Last, two other pathways are activated : the TGF-β and the Wnt signaling pathways. Regarding the TGF-β pathway, 22 genes were upregulated vs 3 downregulated. The transforming growth factor receptor R1, Tgfbr1, is also upregulated (2.25 fold). Concerning the Wnt pathway,27 genes were upregulated and 9 downregulated. One more time, a membrane receptor is also upregulated, the frizzled class receptor 3 (Fzd3), i.e 3.4 fold. It has to be taken account the signaling pathways involved in metabolism are drastically downregulated. The reactome analysis revealed

the upregulation of genes responsible for the phosphorylation of CREBB1, translation factor involved in the PC12 survival. It has to be noticed the Erk signaling pathway is not upregulated, hence it doesn't seem to be involved in cell survival.

The study of the gene expression profile of PC12 cells on HTMS surface revealed a similar profile to the culture on EDA with the PI3K-Akt signaling pathway activated (**Table 5**). In this case, 40 genes were upregulated and 18 downregulated. The neurotrophin pathways were also activated (23 genes vs 8). The reactome analysis showed that 14 genes leading to NF-KB activation were also upregulated, showing the impact of substrate on cell survival. PC12 cultured on HTMS activated the TGF-β signaling pathway (21 genes upregulated vs 3 downregulated) with the upregulation of the receptor Tgfr1. The Wnt signaling pathway was also activated with 26 genes upregulated and 7 downregulated. Unlike the gene expression on EDA, 3 receptors were upregulated (Fzd1, Fzd3 and Fzd5). In this pathway the downstream effect CREBBP was 2.79 fold upregulated. This factor plays a part in the neuron survival.

Signaling Pathways	Upregulated genes	Downregulated genes
PI3-Akt	47	0
Neurotrophins	27	10
Toll Like Receptors	17	0
Erb	20	8
TGF-β	22	3
Wnt	27	9
Focal Adhesions	30	0

Function	Upregulated genes	Downregulated genes
Filopodia	15	5
Lamellipodia	24	18
Rho GTPase activated Formins	40	4
Microtubule skeleton	34	10
Microtubule cytoskeleton organization	21	3
Microtubule Binding	42	13
Microtubule organization center	31	8
Microtubules	43	22

Table 4: Gene expression profile EDA vs PLL.

Signaling Pathways	Upregulated genes	Downregulated genes
PI3-Akt	40	18
Neurotrophins	23	8
Toll Like Receptors	15	0
Erb	18	6
TGF-β	21	3
Wnt	26	7
Focal Adhesions	26	0

Function	Upregulated genes	Downregulated genes
Rho GTPase activated Formins	37	3
Microtubule skeleton	31	9
Microtubule cytoskeleton organization	22	3
Microtubule Binding	40	8
Microtubule organization center	5	0
Microtubules	41	19

Table 5: Gene expression profile HTMS vs PLL.

3.6 Regulation of genes involved in the neurite formation

PC12 cultivated on EDA upregulated 30 genes involved in focal adhesions (compared to the cell culture on PLL). Among them, Rock1 and Rock 2 were dramatically overexpressed. Focal adhesions

are generated during neurite formation at the growth cone level to stabilize it. In addition, several effectors activating Rho GTPase, enzyme required in the formation of focal adhesion are upregulated. For instance, 40 genes involved in RhoGTPase activated formins are upregulated. Besides, 32 vs 16 genes involved in the actin cytoskeleton regulation are upregulated. The growth cone is characterized by the generation of filopodia and lamellipodia. Regarding lamellipodia, 24 genes were upregulated and 18 downregulated. For the filopodia, 15 were upregulated and 5 downregulated. Among them, cdc 42 and rac1 are overexpressed. Taken together, the gene expression profile is more toward the growth cone formation.
The neurite growth also requires the involvement of the tubulin receptor to extend the neurite length. The Go analysis of the microarray showed that 43 vs 22 genes involved in microtubule formation were upregulated. Moreover, 31 vs 8 genes involved in the microtubule organization centers were also upregulated. Last, 21 genes responsible for the microtubule organization were upregulated vs 8 downregulated.
The PC12 cells upregulated 26 genes involved in the focal adhesion formation when they were cultivated on HTMS. Hence, the gene expression was similar to that on EDA. Rock1, Rock 2 and cdc 42 were also upregulated as well as Rho GTPase activators. Regarding the microtubule formation, 41 genes were upregulated versus 19 and genes involved in microtubule formation (40 vs 8) and microtubule organization (31 vs 9) too. This evidenced the similar behavior of PC12 cells in contact to HTMS compared to EDA surfaces.

3.7 Effect of K-252a on neurite outgrowth for PC12 cells cultured on EDA and HTMS

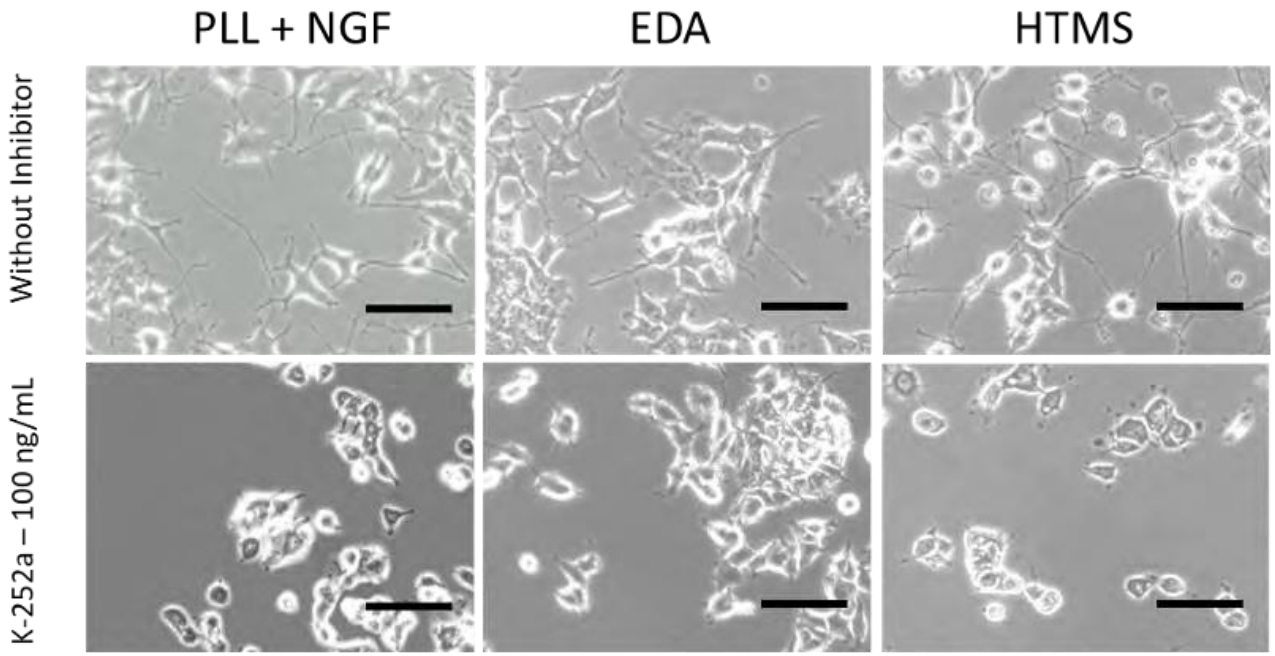

Figure 6: Effect of K252a (100 $ng\ mL^{-1}$) on PC12 morphology and neurite outgrowth after 72h of culture on the different substrates. Bar : 50 μm.

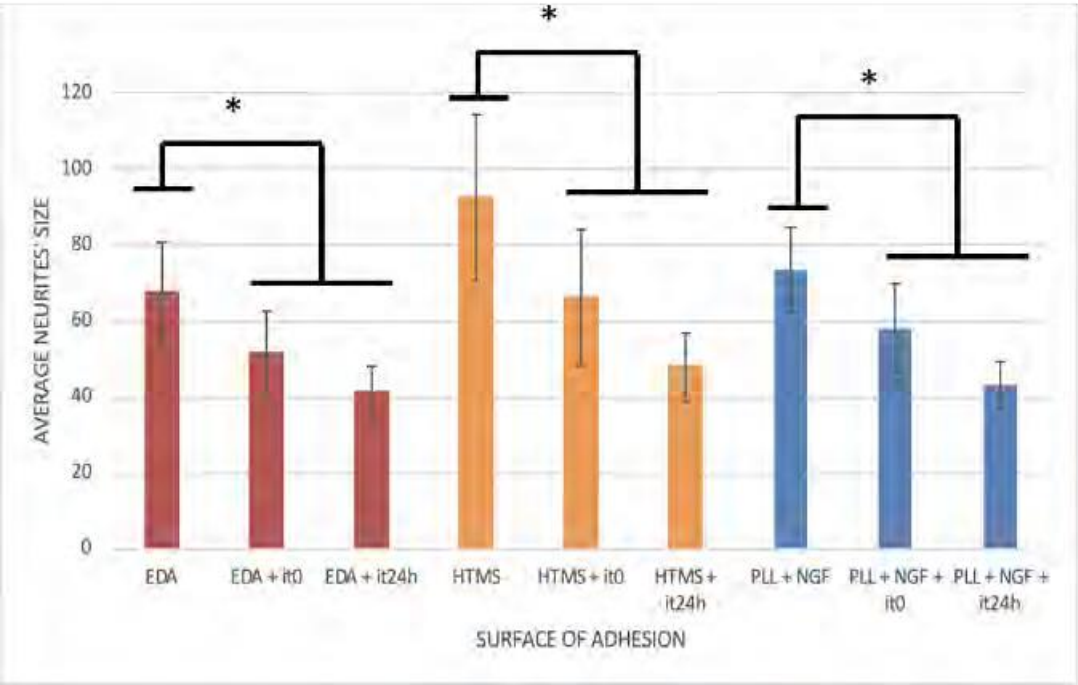

Figure 7: Effects of the inhibitor K252a treatment on PC12 neurite length on different surfaces.Cells were treated by $C_{K252a} = 100\ nM$. (Red) Cells cultivated on EDA surfaces. (Yellow) Cells cultivated on HTMS surfaces. (Blue) Cells cultivated on PLL + NGF surfaces. *: $p < 0.05$, Mann-Whitney test. for the legend : it_x: i stands for inhibitor, t_0 and t_{24h} refer to the timing for both experiments. Addition of the inhibitor was added on day 0 and again on day 1 ($24h$) (see Table 2).

Two different inhibitor concentrations were used for each modified surface, *i.e* 10 *nM* and 100 *nM* . The use of the concentration 10 nM (Figure 1 in Supporting Information) of the inihibtor on PC12 cells shows that the neurite formation is not totally inhibited. Using 100 nM,, the neurite growth was inhibited by around 50% in all conditions, *i.e* on EDA, HTMS and PLL+NGF (Figure 7).

3.8 Effect of EDA and HTMS surfaces on cytoskeleton and growth cone formation detected by immunfluorescence

In order to visualize the impact of the 4 different culture substrates, *i.e* PLL, PLL plus NGF, HTMS and EDA on the cell behavior of PC12, we performed experiments of immunohistochemistry showing the localization of Tubulin and Actin (Figure 8), the major proteins involved in the neuronal cytoskeleton. Neuromodulin (GAP-43), a neurospecific calmodulin binding protein was also detected to observe neuronal growth. The main objective of this study was to confirm at the protein level the cell behavior observed at the transcriptional level. PC12 cells cultured on HTMS, EDA and PLL+NGF exhibited a high alpha tubulin production in the neurites (Figure 8D, 8G and 8J). In contrast, the alpha tubulin labelling was located around the nucleus in PC12 cells cultured on PLL substrates (Figure 8A). No neurites were observable in this condition. GAP-43 labelling was localized in the membrane level, at the cell extremity when cells were cultured on HTMS, EDA and PLL+NGF (Figure 8E, 8H and 8K). On the opposite, a weak signal of GAP-43 was detected around the cell nucleus of PC12 cultivated on PLL surfaces (Figure 8B). Actin was barely observed in the cell body of PC12 cultured on PLL (Figure 8C). No stress fiber was visible. Regarding the functionalized surfaces HTMS and EDA, actin was located through in the cell body but also at the cell extremity with a more intense labelling (Figure 8F and 8I). PC12 cultured on PLL+NGF exhibited the same features (Figure 8L).

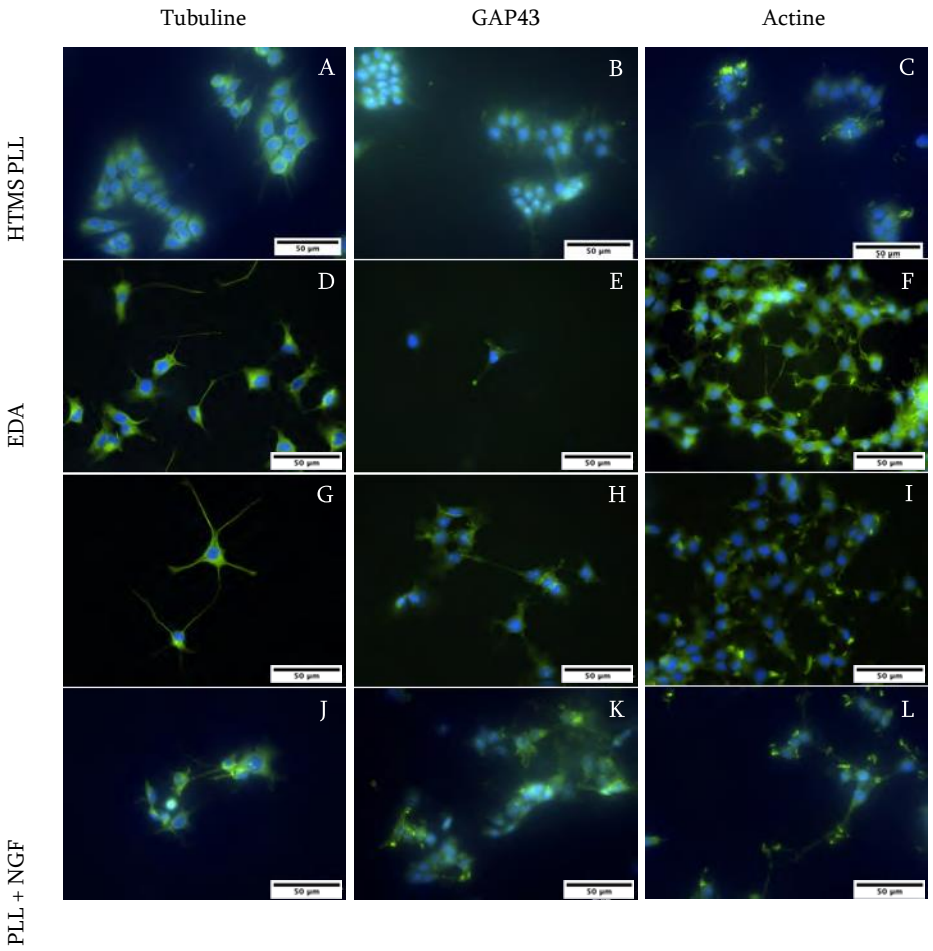

Figure 8: Effect of functionalized surfaces on neurite formation revealed by immunofluorescence. Tubulin actin and neuromodulin (GAP-43) were detected in PC12 cells cultivated on PLL, EDA and HTMS surfaces.

4 Discussion

The present study aimed to unravel the molecular mechanisms involved in the neurite outgrowth of neuronal-like PC12 cells under the effect of gradients in the surface force field (*i.e.* the spatial distribution of the adhesion energy).

It arises after analysis of the experimental results that the molecular mechanism is indistinguishable from that identified for the action of the nerve growth factor NGF on PC12 cells reported in the literature. The differentiation process is independent of the chemical nature of the molecules which generate the gradient in the adhesion energy and of the amplitude of the gradient. Indeed, the gradient generated with HTMS is approximately 1.5 fold greater than that with EDA. The only relevant physical parameter for differentiation is the existence of these local gradients, this is the second strong point that emerges from this investigation. We have produced culture substrates by specific chemical treatment of clean glass surfaces in order to obtain a physical nanostructure generating local surface energy gradients. The behavior of PC12 cells has been analyzed on such surfaces which initiate the neurite outgrowth in the absence of chemical stimulation by NGF. The outgrowth of neurites and the expression of neuronal genes indicate that the physical surface signals act in the same way than the chemical treatment with NGF. The physical parameter which is the surface energy gradient is detected by the filopodia and transduced-translated as a signaling pathway leading to differentiation. As confirmed in our previous work, PC12 cells adhere well to surfaces exhibiting heterogeneity induced by chemisorption of EDA and HTMS. [4, 31] This

leads to the appearance of a local adhesion energy gradient which therefore seems to promote cell adhesion. [4,31] The surfaces modified by "HTMS" are without electrical charges, which then allows us to emphasize that the neuritogenesis observed is independent of the presence of surface electrical charges. If the effect of electric charges took place, it would have been predominant PLL surfaces were used since they are ionized in the culture medium.

Neurite formation begins with the accumulation and the organization of actin and microtubule cytoskeleton to generate a growth cone [50]. The growth starts with the filopodia appearance, followed by their enlargement to create a lamellipodia. [51] Several external cues drive neurite outgrowth. Among them, the neurotrophic factors such as NGF promote assembly and disassembly of cytoskeleton structure to induce neurite formation . [52] The binding of NGF on its receptor TrkA leads to the activation of the PI3K/Akt signaling pathway which modulate the neuronal plasticity by favoring the filopodia and lamellipodia formation . [50] The culture of PC12 cells on EDA or HTMS substrate led to the neurite formation after 72 *h* in culture and this outgrowth was correlated to the upregulation of genes involved in this PI3K/Akt signaling pathway. Interestingly, the contact of cells on these supports did not trigger the expression of NGF. These results were confirmed by the microarray as these neurotrophic factors were not overexpressed compared to the control condition which did not exhibit any neurite (PC12 cultured on Polylysine surface). Hence the contact of PC12 cells on these substrates activated this signaling pathway possibly by directly activation of receptors such as TrkA or TrkB. The comparison between the gene expression profile obtained from cells cultured on EDA and HTMS revealed a similar mechanism in term of signaling pathway to promote the neurite formation. EDA and HTMS functionalized surfaces are different, EDA surface is hydrophilic whereas HTMS is hydrophobic. In addition, they exhibit energy gradients with different amplitude. However, the existence of a gradient is the main stimulus to activate the PI3/Akt pathway and the neurite formation. With the aim of investigating the activation of the NGF receptor by the energy gradient, K252a, a TrkA inhibitor, was added to the PC12 cultured on EDA and HTMS without addition of NGF. The inhibitor decreased by 50% the neurite outgrowth after 3 days of culture, thereby evidencing the predominant role of TrkA activation in the signal transduction generated by the surface energy gradient.

Beside its role in neuritogenesis, the PI3/Akt pathway also plays a crucial role in cell survival via activation of the MAP kinase pathway . [53] It has to be noticed that this pathway is the only one involved in cell survival. Indeed, the signaling pathway MEK/Erk also involved in cell survival was not modulated by the interactions cells/EDA or cells/HTMS. [54] Last, CREB is upregulated when cells are in contact with EDA and HTMS. This downstream factor of NGF is also involved in cell survival and neuronal plasticity. [55] Taken together, the culture of substrates possessing different energy gradient amplitudes and chemical natures, upregulate the NGF signaling pathway in the same way. This suggests the existence of a threshold value of this energy gradient to trigger neurite formation. The growth cone generation requires the formation of focal adhesions to stabilize it and to allow the neurite growth . [56,57] Regardless of the substrate studied, gene involved in signaling pathway leading to focal adhesion were upregulated. One more time, the energy gradient provides the external cues to activate signaling pathways to form philopodia and lamellipodia. Beside the actin or microtubule polymerization, the formation of neurites requires the expression of proteins stabilizing and destabiliz- ing cytoskeleton. As an example, microtubules bundles are stabilized by associated protein to stabilize them during neuritogenesis. In addition, an interaction between both cytoskeletons is also crucial. [50] Cdc 42 and Rac 1 are the two main downstream effectors which allow for the formation of filopodia and lamellipodia. [58] Cdc 42 was upregulated in cells in contact with EDA or HTMS. This result is quite logical as cdc 42 is a downstream effector of the PI3K/Akt pathway. [59] The analysis of gene expression by the Go analysis focusing on gene function revealed that a lot of proteins involved in the microtubule organization, polymerization and binding with the actin cytoskeleton were upregulated. This shows the positive impact of EDA and HTMS on the neurite growth by promoting the formation of required cytoskeletal structure. These results were confirmed at the protein level with the immun- odetection of alpha tubulin, actin and GAP43. Cells cultivated on EDA and HTMS produced large quantities of tubulin at the neurite level. Actin was localized at the cell extremities and GAP43 at the growth cone level. In contrast, GAP43 was not detected in PC12 cells cultivated on PLL, thereby showing the absence of neuritogenesis.

Effectors such as Rock 1 and Rock 2 were also overexpressed when PC12 cells were cultivated on these substrates. These proteins under the control of Rho –GTPases such as Rho A are negative control of neuritogenesis by promoting the formation of stress fibers and inhibiting the formation of filopodia. [60] Rock 1 and 2 are downstream effectors of the TGF-β and Wnts signaling pathways. Regarding the latter, this effect is the consequence of the binding of Wnts on their Frizzled receptors. PC12 cultured on EDA

and HTMS upregulated a lot of genes involved in these signaling pathways. [61] In addition, some receptors involved in these pathways were also upregulated. As a

consequence, the contact with EDA and HTMS also upregulate signaling pathways which negatively impact the neurite growth. Nevertheless, it is a minor effect as it did not prevent the cone growth and the neurite formation. In addition, no stress fiber (after actin labeling) was visible within PC12 cells cultured on HTMS and EDA surfaces.

5 Conclusion

In this study, the biological mechanism leading to neurite growth and cell differentiation of PC12 cells cultured on surfaces possessing a gradient of surface energy has been elucidated. The distribution of the surface energy at the origin of the neurite formation mainly activates the signaling pathways PI3/Akt which promotes cell survival and growth cone formation. Surface energy gradients act on cell via activation of the NGF receptor TrkA, thereby mimicking the effect of this growth factor in vivo. These surfaces afford an ongoing activation of neuronal differentiation which avoids the sequential addition of NGF into the milieu . Taken together, these results show that functionalized surface with energy surface gradients could be useful for an application to promote nerve repair after an injury.

6 Raw data management

Regarding the microarray, the raw data were uploaded to the website GEO under the reference number : *GSE*208126. The reader can access to the entire files with the link : https://www.ncbi.nlm.nih.gov/gds Raw Data

7 Acknowledgements

All the authors contributed equally, they carried out the measurements, contributed to the design and implementation of the research, to the analysis of the results and to the writing of the manuscript. The present study was supported by Grant from French ministry of Research (Ecole Doctorale 397), CNRS, Sorbonne Université and Université Paris Descartes. Thanks are due to *Cochin Institute* for assistance and F. Semprez and K. Gouffaud for their help in cell culture. Last we acknowledge GENOSPLICE for their analysis on the microarray.

Conflict of interest
The authors declare no conflict of interest

References

[1] Y.W. Fan, F.Z. Cui, S.P. Hou, Q.Y. Xu, L.N. Chen, and I.-S. Lee. Culture of neural cells on silicon wafers with nano-scale surface topograph. *Journal of Neuroscience Methods*, 120(1):17–23, 2002.

[2] Ying Xiong, Aih Cheun Lee, Daniel M. Suter, and Gil U. Lee. Topography and nanomechanics of live neuronal growth cones analyzed by atomic force microscopy. *Biophysical Journal*, 96(12):5060– 5072, 2009.

[3] Guillaume Lamour, Nathalie Journiac, Sylvie Souès, Stéphanie Bonneau, Pierre Nassoy, and Ahmed Hamraoui. Influence of surface energy distribution on neuritogenesis. *Colloids and Surfaces B: Biointerfaces*, 72(2):208–218, 2009.

[4] Guillaume Lamour, Ali Eftekhari-Bafrooei, Eric Borguet, Sylvie Souès, and Ahmed Hamraoui. Neuronal adhesion and differentiation driven by nanoscale surface free-energy gradients. *Bioma- terials*, 31(14):3762–71, May 2010.

[5] Weiqiang Chen, Shuo Han, Weiyi Qian, Shinuo Weng, Haiou Yang, Yubing Sun, Luis G Villa-Diaz, Paul H Krebsbach, and Jianping Fu. Nanotopography regulates motor neuron differentiation of human pluripotent stem cells. *Nanoscale*, 10(7):3556–3565, Feb 2018.

[6] Claire Leclech and Catherine Villard. Cellular and subcellular contact guidance on microfabricated substrates. *Front Bioeng Biotechnol*, 8:551505, 2020.

[7] James Q. Zheng. Turning of nerve growth cones induced by localized increases in intracellular calcium ions. *Nature*, 403(6765):89–93, 2000.

[8] K Hong, M Nishiyama, J Henley, M Tessier-Lavigne, and M Poo. Calcium signalling in the guidance of nerve growth by netrin-1. *Nature*, 403(6765):93–98, Jan 2000.

[9] V H Höpker, D Shewan, M Tessier-Lavigne, M Poo, and C Holt. Growth-cone attraction to netrin-1 is converted to repulsion by laminin-1. *Nature*, 401(6748):69–73, Sep 1999.

[10] S McFarlane. Attraction vs. repulsion: the growth cone decides. *Biochem Cell Biol*, 78(5):563–568, 2000.

[11] Makoto Nishiyama, Akemi Hoshino, Lily Tsai, John R Henley, Yoshio Goshima, Marc Tessier-Lavigne, Mu-Ming Poo, and Kyonsoo Hong. Cyclic amp/gmp-dependent modulation of ca2+ channels sets the polarity of nerve growth-cone turning. *Nature*, 423(6943):990–995, Jun 2003.

[12] Ulrich S. Schwarz and Ilka B. Bischofs. Physical determinants of cell organization in soft media. *Medical Engineering and Physics*, 27(9):763–772, 2005. This issue contains a special section on Effects of Mechanical Forces Engineering Reactions at the Cellular Level.

[13] Paul C. Letourneau. Cell-to-substratum adhesion and guidance of axonal elongation. *Developmental Biology*, 44(1):92 – 101, 1975.

[14] J A Hammarback and P C Letourneau. Neurite extension across regions of low cell-substratum adhesivity: implications for the guidepost hypothesis of axonal pathfinding. *Dev Biol*, 117(2):655– 662, Oct 1986.

[15] P C Letourneau. Possible roles for cell-to-substratum adhesion in neuronal morphogenesis. *Dev Biol*, 44(1):77–91, May 1975.

[16] D.A. Stenger, C.J. Pike, J.J. Hickman, and C.W. Cotman. Surface determinants of neuronal survival and growth on self-assembled monolayers in culture. *Brain Research*, 630(1):136–147, 1993.

[17] D Kleinfeld, KH Kahler, and PE Hockberger. Controlled outgrowth of dissociated neurons on patterned substrates. *Journal of Neuroscience*, 8(11):4098–4120, 1988.

[18] Ravi Kapur and Alan S. Rudolph. Cellular and cytoskeleton morphology and strength of adhesion of cells on self-assembled monolayers of organosilanes. *Experimental Cell Research*, 244(1):275– 285, 1998.

[19] Chaim N. Sukenik, Natarajan Balachander, Lloyd A. Culp, Kristine Lewandowska, and Katherine Merritt. Modulation of cell adhesion by modification of titanium surfaces with covalently attached self-assembled monolayers. *Journal of Biomedical Materials Research*, 24(10):1307–1323, 1990.

[20] Tom Wehrman, Xiaolin He, Bill Raab, Abhiram Dukipatti, Helen Blau, and K. Christopher Garcia. Structural and mechanistic insights into nerve growth factor interactions with the trka and p75 receptors. *Neuron*, 53(1):25–38, 2007.

[21] Paul S. Mischel, Joy A. Umbach, Sepehr Eskandari, Shane G. Smith, Cameron B. Gundersen, and Guido A. Zampighi. Nerve growth factor signals via preexisting trka receptor oligomers. *Biophysical Journal*, 83(2):968–976, 2002.

[22] L A Greene and A S Tischler. Establishment of a noradrenergic clonal line of rat adrenal pheochromocytoma cells which respond to nerve growth factor. *Proc Natl Acad Sci U S A*, 73(7):2424–2428, Jul 1976.

[23] Jiang-Zhou Yu and Mark M. Rasenick. Tau associates with actin in differentiating pc12 cells. *The FASEB Journal*, 20(9):1452–1461, 2006.

[24] D G Drubin, S C Feinstein, E M Shooter, and M W Kirschner. Nerve growth factor-induced neurite

outgrowth in PC12 cells involves the coordinate induction of microtubule assembly and assembly-promoting factors. *Journal of Cell Biology*, 101(5):1799–1807, 11 1985.

[25] Ninel Azoitei, Thomas Wirth, and Bernd Baumann. Activation of the ikb kinase complex is sufficient for neuronal differentiation of pc12 cells. *Journal of Neurochemistry*, 93(6):1487–1501, 2005.

[26] DK Fujii, SL Massoglia, N Savion, and D Gospodarowicz. Neurite outgrowth and protein synthesis by pc12 cells as a function of substratum and nerve growth factor. *Journal of Neuroscience*, 2(8):1157–1175, 1982.

[27] Jerome R. Wujek and Richard A. Akeson. Extracellular matrix derived from astrocytes stimulates neuritic outgrowth from pc12 cells in vitro. *Developmental Brain Research*, 34(1):87–97, 1987.

[28] Christine E. Schmidt, Venkatram R. Shastri, Joseph P. Vacanti, and Robert Langer. Stimulation of neurite outgrowth using an electrically conducting polymer. *Proceedings of the National Academy of Sciences*, 94(17):8948–8953, 1997.

[29] Arundhati Kotwal and Christine E Schmidt. Electrical stimulation alters protein adsorption and nerve cell interactions with electrically conducting biomaterials. *Biomaterials*, 22(10):1055–1064, 2001. Neural Tissue Engineering.

[30] Yi Guo, Mengyan Li, Andreas Mylonakis, Jingjia Han, Alan G. MacDiarmid, Xuesi Chen, Peter I. Lelkes, and Yen Wei. Electroactive oligoaniline-containing self-assembled monolayers for tissue engineering applications. *Biomacromolecules*, 8(10):3025–3034, 10 2007.

[31] Guillaume Lamour, Sylvie Souès, and Ahmed Hamraoui. Substrate-induced pc12 cell differentiation without filopodial, lamellipodial activity or ngf stimulationa. *Macromolecular Bioscience*, 15(3):364–371, 2015.

[32] Murnane Aeneas C., Brown Kimberly, and Keith Charles H. Preferential initiation of pc12 neurites in directions of changing substrate adhesivity. *Journal of Neuroscience Research*, 67(3):321–328, 2002.

[33] John D. Foley, Eric W. Grunwald, Paul F. Nealey, and Christopher J Murphy. Cooperative modulation of neuritogenesis by pc12 cells by topography and nerve growth factor. *Biomaterials*, 26(17):3639–3644, June 2005.

[34] Furqan Haq, Venkatramani Anandan, Charles Keith, and Guigen Zhang. Neurite development in pc12 cells cultured on nanopillars and nanopores with sizes comparable with filopodia. *Int J Nanomedicine*, 2(1):107–115, 2007.

[35] B Arkles. Tailoring surfaces with silanes. *Chemtech*, 7(12):766, 1977.

[36] Limin Wang, Ulrich S. Schubert, and Stephanie Hoeppener. Surface chemical reactions on self-assembled silane based monolayers. *Chem. Soc. Rev.*, 50:6507–6540, 2021.

[37] Guillaume Lamour, Ahmed Hamraoui, Andrii Buvailo, Yangjun Xing, Sean Keuleyan, Vivek Prakash, Ali Eftekhari-Bafrooei, and Eric Borguet. Contact angle measurements using a simplified experimental setup. *Journal of Chemical Education*, 87(12):1403–1407, 2010.

[38] Robert J. Good and L. A. Girifalco. A theory for estimation of surface and interfacial energies. iii. estimation of surface energies of solids from contact angle data. *The Journal of Physical Chemistry*, 64(5):561–565, 05 1960.

[39] W. A. ZISMAN. *Relation of the Equilibrium Contact Angle to Liquid and Solid Constitution*, chapter 1, pages 1–51. AMERICAN CHEMICAL SOCIETY, WASHINGTON, D.C., 1964.

[40] R. C. Owens, D. K; Wendt. Estimation of the surface free energy of polymers. *JOURNAL OF APPLIED POLYMER SCIENCE*, 13:1741, 1969.

[41] D. Y. Kwok, Y. Lee, and A. W. Neumann. Evaluation of the lifshitz-van der waals/acid-base ap- proach to determine interfacial tensions. 2. interfacial tensions of liquid-liquid systems. *Langmuir*, 14(9):2548–2553,

04 1998.

[42] M W Pfaffl. A new mathematical model for relative quantification in real-time rt-pcr. *Nucleic Acids Res*, 29(9):e45, May 2001.

[43] Pierre de la Grange, Martin Dutertre, Natalia Martin, and Didier Auboeuf. FAST DB: a website resource for the study of the expression regulation of human gene products. *Nucleic Acids Research*, 33(13):4276–4284, 01 2005.

[44] Pierre de la Grange, Martin Dutertre, Margot Correa, and Didier Auboeuf. A new advance in alternative splicing databases: from catalogue to detailed analysis of regulation of expression and function of human alternative splicing variants. *BMC Bioinformatics*, 8(1):180, 2007.

[45] Pierre de la Grange, Lise Gratadou, Marc Delord, Martin Dutertre, and Didier Auboeuf. Splicing factor and exon profiling across human tissues. *Nucleic Acids Research*, 38(9):2825–2838, 01 2010.

[46] Robin Haw and Lincoln Stein. Using the reactome database. *Current Protocols in Bioinformatics*, 38(1):8.7.1–8.7.23, 2012.

[47] Da Wei Huang, Brad T Sherman, and Richard A Lempicki. Systematic and integrative analysis of large gene lists using DAVID bioinformatics resources. *Nature Protocols*, 4(1):44–57, dec 2008.

[48] Arthur W. Adamson and Alice P. Gast. *Physical Chemistry of Surfaces*. A WILEY- INTERSCIENCE PUBLICATION, 6 edition, 1997.

[49] A. Bose. Wetting by solutions. In J. C. Berg, editor, *Wettability*, volume 49 of *Surfactant Science*, chapter 3, page 149. CRC Press, 1993.

[50] Rajiv Sainath and Gianluca Gallo. Cytoskeletal and signaling mechanisms of neurite formation. *Cell and Tissue Research*, 359(1):267–278, jul 2014.

[51] Erik W Dent and Frank B Gertler. Cytoskeletal dynamics and transport in growth cone motility and axon guidance. *Neuron*, 40(2):209–227, oct 2003.

[52] Jorge A Sierra-Fonseca, Omar Najera, Jessica Martinez-Jurado, Ellen M Walker, Armando Varela-Ramirez, Arshad M Khan, Manuel Miranda, Nazarius S Lamango, and Sukla Roychowdhury. Nerve growth factor induces neurite outgrowth of PC12 cells by promoting g$\beta\gamma$-microtubule in- teraction. *BMC Neuroscience*, 15(1), dec 2014.

[53] Hui-Zhi Long, Yan Cheng, Zi-Wei Zhou, Hong-Yu Luo, Dan-Dan Wen, and Li-Chen Gao. PI3k/AKT signal pathway: A target of natural products in the prevention and treatment of alzheimer's disease and parkinson's disease. *Frontiers in Pharmacology*, 12, apr 2021.

[54] Prashant Kumar Modi, Narayana Komaravelli, Neha Singh, and Pushkar Sharma. Interplay between MEK-ERK signaling, cyclin d1, and cyclin-dependent kinase 5 regulates cell cycle reentry and apoptosis of neurons. *Molecular Biology of the Cell*, 23(18):3722–3730, sep 2012.

[55] Steven Finkbeiner, Sohail F Tavazoie, Anna Maloratsky, Kori M Jacobs, Kristen M Harris, and Michael E Greenberg. CREB: A major mediator of neuronal neurotrophin responses. *Neuron*, 19(5):1031–1047, nov 1997.

[56] Phillip R. Gordon-Weeks. *Neuronal Growth Cones*. Developmental and Cell Biology Series. Cambridge University Press, 2000.

[57] Jonathan P. Myers and Timothy M. Gomez. Focal adhesion kinase promotes integrin adhesion dynamics necessary for chemotropic turning of nerve growth cones. *Journal of Neuroscience*, 31(38):13585–13595, 2011.

[58] Hironori Katoh, Hidekazu Yasui, Yoshiaki Yamaguchi, Junko Aoki, Hirotada Fujita, Kazutoshi Mori, and Manabu Negishi. Small GTPase RhoG is a key regulator for neurite outgrowth in PC12 cells. *Molecular and Cellular Biology*, 20(19):7378–7387, oct 2000.

[59] Kazuhiro Aoki, Takeshi Nakamura, and Michiyuki Matsuda. Spatio-temporal regulation of rac1 and cdc42 activity during nerve growth factor-induced neurite outgrowth in pc12 cells*. *Journal of Biological Chemistry*, 279(1):713–719, 2004.

[60] Linda Julian and Michael F Olson. Rho-associated coiled-coil containing kinases (ROCK). *Small GTPases*, 5(2):e29846, apr 2014.

[61] Alice H Chou and Bruce D Howard. Inhibition by wnt-1 or wnt-3a of nerve growth factor-induced differentiation of PC12 cells is reversed by bisindolylmaleimide-i but not by several other PKC inhibitors. *Oncogene*, 21(41):6348–6355, sep 2002.